



# Lifetime of MoS<sub>2</sub> based DFL systems in fretting with and without a Cu-Ni-In under-layer: The dependence on the topography of the surface onto which the DFL is deposited

E. Laolu-Balogun<sup>a</sup>, S. Owen<sup>b</sup>, T. Booth<sup>b</sup>, G. Pattinson<sup>b</sup>, P.H. Shipway<sup>a</sup>, K.T. Voisey<sup>a,\*</sup>

<sup>a</sup> Faculty of Engineering, University of Nottingham, NG7 2RD, United Kingdom

<sup>b</sup> Rolls-Royce plc, Derby, United Kingdom

## ARTICLE INFO

### Keywords:

Dry film lubricant  
Fretting  
Surface topography  
Molybdenum disulphide  
Cu-Ni-In

## ABSTRACT

The superior fretting performance of polymer-bonded MoS<sub>2</sub>-based dry film lubricant (DFL) coating on a plasma-sprayed Cu-Ni-In under-layer is well known. The Cu-Ni-In under-layer changes both the material and the topography of the surface onto which the DFL is applied. However, the mechanism of how the DFL/Cu-Ni-In interface improves fretting performance requires further investigation. Here, the effects of material and roughness were isolated by using surfaces with the Cu-Ni-In under-layer coating and the Ti-6Al-4 V substrate in both the ground and grit-blasted conditions. Increasing Cu-Ni-In surface roughness from 1 μm to 9 μm more than doubled fretting lifetime. The Cu-Ni-In under-layer is shown to provide added durability and extended lifetimes, over fivefold, when compared to Ti-6Al-4 V substrate despite having similar surface topographies.

## 1. Introduction

Fretting wear is associated with the removal of material from a contact between two contacting surfaces by small oscillatory movements [1] which can vary in frequency, amplitude and applied normal load across the contact [2]. This form of material degradation remains a problem in many industrial settings, including that of dovetail joints of aero-engine fan blades, where the effects of fretting can be particularly damaging due to wide variations in the operating conditions coupled with the poor tribological properties of the titanium alloys from which such systems are commonly fabricated [3,4]. To actively prolong the lifetimes of fan blades, current industrial practices to ameliorate the effects of fretting include a complex surface engineering solution where the fan blade dovetail is shot peened and then plasma spray coated with a copper-nickel-indium (Cu-Ni-In) alloy coating (with a typical Ra value of ~ 9 – 10 μm [5–8]), onto which a polymer-bonded molybdenum disulphide (MoS<sub>2</sub>)-based solid lubricant coating is then deposited [9,10]. This surface engineering architecture is thought to provide dual advantages for the fretting system owing to the accommodating capacity of plastic deformation provided by the Cu-Ni-In coating, which limits the nucleation and propagation of cracks, and the low friction and low wear properties of the solid lubricant coating itself [11,12].

The degradation process of polymer-bonded MoS<sub>2</sub> solid lubricant in

fretting wear has been shown to exhibit a first stage where the coating undergoes plastic deformation. During this stage, the asperity peaks of the coatings are sheared off and the lubricating particles flow to form a continuous debris flow layer [13]. Following this, micro-cracks initiate and propagate in the coatings with the detachment of particles from the surfaces resulting in the progressive elimination of the coating along with the oxidation of the MoS<sub>2</sub>. Final failure occurs with severe detachment of the coating layers where metallic asperities emerge through the coating, making direct contact with the metallic counter-face, resulting in high coefficient of friction [14–17].

Xu et al. [18] performed a series of fretting wear tests to investigate the life of bonded MoS<sub>2</sub> solid lubricant coatings deposited directly onto steel substrates with different substrate hardness (~ 275 HV and ~440 HV) and surface roughness, (Ra of 0.5 μm and 2.0 μm). Against their criterion of failure (based upon the coefficient of friction reaching a value of 0.25), they observed an increase in lifetime of the heat cured DFL of ~ 10% on changing from the softer to the harder steel substrate for fretting displacement amplitudes of both 20 μm and 40 μm. A similar increase in lifetime of the heat cured DFL of ~ 10% was observed on increasing the surface roughness of the (harder) substrate onto which the DFL was deposited. It was suggested that rougher substrates resulted in an increase in bond strength between the coating and the substrate as well as being effective against wear in the later stages of fretting due to

\* Corresponding author.

E-mail address: [katy.voisey@nottingham.ac.uk](mailto:katy.voisey@nottingham.ac.uk) (K.T. Voisey).

<https://doi.org/10.1016/j.triboint.2023.108863>

Received 19 June 2023; Received in revised form 28 July 2023; Accepted 6 August 2023

Available online 7 August 2023

0301-679X/© 2023 The Authors. Published by Elsevier Ltd. This is an open access article under the CC BY license (<http://creativecommons.org/licenses/by/4.0/>).

residual MoS<sub>2</sub> being retained in the troughs of the rough surface.

More recently, others have drawn similar conclusions regarding the role of the roughness of the substrate onto which the DFL is deposited [15,19]. Barman et al. [15] presented data related to wear profiles at various stages of damage of a system where a nominally 50 µm thick DFL had been deposited onto grit-blasted Ti-6Al-4 V; these profiles have been used to make an estimate of the wear depth as a function of the exposure to wear which is presented in Fig. 1. It can be seen that the rate of increase of penetration is high as the DFL itself is worn away, but that this is followed by an extended period (~ 20 – 40 × 10<sup>3</sup> cycles) where the rate of penetration is low; it was argued that this is associated with the period where the wearing surface is made up of a mix of metal and DFL and is a significant period in the lifetime of the system.

The presence of the Cu-Ni-In layer in the surface engineered system architecture is thought to alter the fretting contact configuration as it is less stiff and less resistant to plastic deformation than the fan blade material, with an elastic modulus of 60 GPa and a Vickers hardness of 170 HV compared to 119 GPa and 360 HV respectively for the Ti-6Al-4 V blade [20]. By conducting fretting wear tests on unlubricated self-mating Ti-6Al-4 V surfaces with a hardness of 284 HV, an elastic modulus of 143 GPa and a roughness (Ra) of 0.1 µm and then on Ti-6Al-4 V mated against Cu-Ni-In which had a lower hardness and elastic modulus of 138 HV and 90 GPa respectively and a higher surface roughness (Ra) of around 9 µm, Hager et al. [6] observed comparable coefficients of friction within the two systems that ranged between 0.68 and 0.85. However, less short-term variation in the friction coefficient (and hence, greater stability) was observed for the system where one of the components had the Cu-Ni-In coating.

It is well established that DFLs of this type typically confer extended lifetimes before failure when deposited onto thermally sprayed Cu-Ni-In. The implications of a Cu-Ni-In under-layer below polymer-bonded MoS<sub>2</sub> dry film lubricants were explored by Barman et al. [5] who sought to uncover the specific role that a thermally sprayed Cu-Ni-In layer plays on the tribological performance in Ti-6Al-4 V dovetail arrangements. In that work, a MoS<sub>2</sub> DFL was applied either on top of a thermally sprayed Cu-Ni-In coating or directly to a grit-blasted Ti-6Al-4 V substrate. The soft metallic layer of Cu-Ni-In (177 ± 20 HV) displayed significantly higher roughness (Ra) of 9.0 µm compared to that of the harder (287 ± 10 HV) grit-blasted Ti-6Al-4 V substrate with a Ra of 2 µm. The MoS<sub>2</sub> DFL exhibited significantly enhanced durability when applied on top of the Cu-Ni-In coating, with a five-fold increase in lifetime typically being observed. It was suggested that the high roughness resulted in an extended lifetime for the phase of wear where the contacting surface experiencing fretting motion was partly made up of metal and partly of DFL itself, with this mixed material exhibiting high resistance to degradation and wear. It was argued that the increased lifetime with increasing roughness could be explained by the concept of the mixed

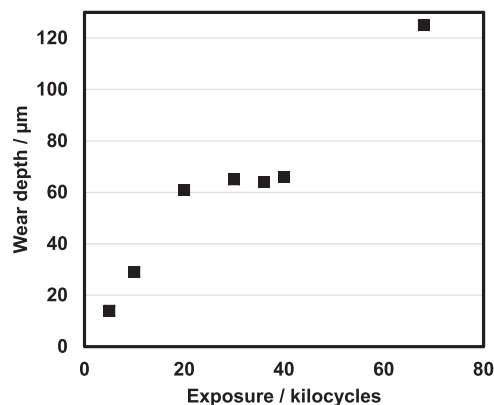


Fig. 1. Wear depth as a function of exposure to fretting wear for a nominally 50 µm thick DFL deposited onto a grit-blasted Ti-6Al-4 V substrate [15].

metal-DFL simply existing over an extended depth of penetration by the wear process.

Fouvry et al. [21] conducted fretting wear tests between (i) a Cu-Ni-In coated substrate, itself coated with bonded MoS<sub>2</sub> and (ii) an uncoated, shot peened Ti-6Al-4 V counter-body; they observed that the intrinsic wear resistance of the MoS<sub>2</sub> coating is controlled by the damage process activated within the interface. Increased titanium transfer from the Ti-6Al-4 V counter-body was triggered by high pressure conditions which promoted seizure, severe abrasive wear, and an increased wear rate of the bonded MoS<sub>2</sub> coating along with a sharp increase in friction coefficient. At lower contact pressures, minimal activation of titanium transfer was observed at the Cu-Ni-In fretting interface which instead gave way to the progressive elimination and oxidation of the bonded MoS<sub>2</sub> coating leading to a more stable and gradual increase in friction coefficient.

There is a need to understand the dominant mechanisms behind the extended lifetimes that are observed when thermally sprayed Cu-Ni-In is employed as an under-layer in the application of a DFL to a Ti-6Al-4 V component. It is noted that there are many differences between a thermally sprayed Cu-Ni-In surface and a prepared Ti-6Al-4 V surface for deposition of a DFL, with these being broadly categorised as (i) differences in topography (roughness); (ii) differences in the nature of the materials (such as chemical affinity for the DFL, hardness and Young's modulus etc.). To identify the dominant causal mechanism, the aim of this work is to isolate the separate effects of surface material type and surface topography to understand their distinct influences to aid the optimisation of anti-fretting systems.

## 2. Experimental methodology

A cylinder-on-flat fretting contact configuration was employed as indicated in Fig. 2. This resulted in a contact length ( $w$ ) of 10 mm (determined by the width of the flat sample) with the cylindrical sample having a radius,  $R$ , of 15 mm. Fretting tests were conducted with samples fabricated from Ti-6Al-4 V to represent the material comprising the fan blade and disc in an aero-engine dovetail joint.

The surface treatments were applied to match current industrial practices for fan blade and disc counterparts of the fan blade dovetail joint [7,10]. Accordingly, both cylindrical and flat samples for the fretting pairs were machined from a Ti-6Al-4 V plate which is reported to have an elastic modulus of 115 GPa and a Poisson's ratio of 0.342 [5]. For selected Ti-6Al-4 V flat samples, the substrate specimen was first shot peened, grit-blasted and then plasma sprayed with a Cu-Ni-In layer with an approximate thickness of 100–190 µm by an external contractor. Plasma spraying was conducted with a gas atomised feedstock powder (Metco 58 supplied by Oerlikon Metco) with a nominal composition of 59 wt% copper, 36 wt% nickel and 5 wt% indium and a nominal size distribution of – 75 + 46 µm, indicating that 90% of the particles lie in this size range. An equivalent plasma-sprayed Cu-Ni-In layer has been shown to have an elastic modulus of 66 GPa and a Poisson's ratio of 0.15 [21]. Vickers micro-hardness tests (with a 200 gf load) have shown that

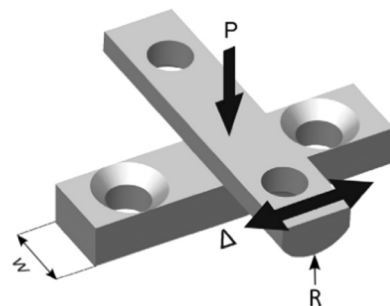


Fig. 2. Cylinder-on-flat specimen configuration used in fretting tests where  $P$  is the applied normal load, and  $\Delta$  is the applied displacement.

the hardness of the Ti-6Al-4 V substrate and the Cu-Ni-In deposit deployed in this work were  $287 \pm 10$  HV and  $177 \pm 20$  HV respectively [5].

Ti-6Al-4 V dovetail joint surfaces are typically shot-peened to promote fretting fatigue strength by introducing residual stresses on the surfaces of the component in order to delay crack initiation and propagation [22]. Accordingly, all the cylindrical samples (uncoated Ti-6Al-4 V) underwent a commercial steel-shot peening process with an intensity of 6–10 A, 230 R shot size and 200% coverage [23] which resulted in a roughness (Sa) of  $0.6 \mu\text{m}$  and a maximum height (Sz) of  $7.3 \mu\text{m}$ .

Mated against this type of cylindrical sample, a range of different fretting couples were made up by use of a flat sample which had one of the surface conditions as detailed in Table 1. Topographical images of the flat surfaces are shown in Fig. 3. Surface characterisation and profilometry was obtained by focus variation microscopy using the Alicona G4 Infinite Focus. A defined area of  $710 \times 539 \mu\text{m}$  was measured for determination of various surface parameters (of the type presented in Table 1) which were calculated in accordance with ISO 25178 using a cut-off wavelength of  $250 \mu\text{m}$  for S-L filters.

In an attempt to de-convolute the effect of material type and surface topography, the as-sprayed Cu-Ni-In surface layer was further processed by both grinding and grit blasting to give a surface topography which was comparable to that of a Ti-6Al-4 V sample which has been similarly prepared. The process of surface grinding involved material removal with successively finer SiC (silicon carbide) grinding paper down to P800, whilst grit-blasting was conducted with aluminium oxide grit (Airblast, UK) with a grit size of  $0.125 - 0.149 \text{ mm}$  with a blast pressure of 3 bar.

Following surface preparation of the flat specimens, a DFL paint was spray deposited on the working surfaces of both the cylindrical and flat fretting samples to align with industrial practice. The DFL was a commercially available epoxy-based paint (procured from Indestructible Paints Ltd, Birmingham, UK under the trade name PL237-R2), in which the primary solid lubricant phase is  $\text{MoS}_2$ . To cure the DFL-coated specimens, they were placed in a circulatory air oven at  $100 \text{ }^\circ\text{C}$ , with the temperature then being increased by  $6 \text{ }^\circ\text{C min}^{-1}$  to  $190 \pm 1 \text{ }^\circ\text{C}$  followed by holding at this temperature for 2 h. Once removed from the oven and cooled to room temperature, the target DFL coating thickness

**Table 1**

Surface processing and surface characteristics of the various forms of the flat fretting specimens onto which the DFL was applied which were employed in the experimental programme.

Surface condition of flat sample in pair	Surface processing applied	Surface roughness (Sa) / $\mu\text{m}$	Maximum height (Sz) / $\mu\text{m}$
As-sprayed Cu-Ni-In	Plasma-spray coated with Cu-Ni-In. No further processing of the as-sprayed coating.	9	84
Grit-blasted Cu-Ni-In	Plasma-spray coated with Cu-Ni-In. Coating then manually ground using SiC papers and then subsequently grit-blasted.	1.0	12
Ground Cu-Ni-In	Plasma-spray coated with Cu-Ni-In. Coating then manually ground using SiC papers.	0.4	4.7
Grit-blasted Ti-6Al-4 V	Uncoated Ti-6Al-4 V sample first ground using a surface grinding machine and then subsequently grit-blasted.	0.9	12.3
Ground Ti-6Al-4 V	Uncoated Ti-6Al-4 V sample ground using a surface grinding machine.	0.5	5.8

( $t$ ) of  $50 \pm 10 \mu\text{m}$  coating thickness was confirmed via an eddy current method using a DeFelsko PosiTector 6000. Due to the complexities of making DFL thickness measurements when deposited onto a Cu-Ni-In interlayer which can affect accuracy, DFL coating procedures were first defined via coating of the flat Ti-6Al-4 V substrate to establish the desired DFL thickness. The same coating process parameters which were used to achieve a thickness of  $50 \pm 10 \mu\text{m}$  on the Ti-6Al-4 V samples were then employed for DFL deposition onto the Cu-Ni-In coated samples. The  $\text{MoS}_2$  particle size in the DFL has been measured at  $2-4 \mu\text{m}$  through examination of high magnification SEM images.

Fretting wear tests were carried out using a servo-hydraulic fretting testing machine; a schematic diagram of the test setup is presented in Fig. 4. In this arrangement, two pairs of identical specimens are fretted simultaneously on the same fixture. A linear variable displacement transducer (LVDT) is mounted to the base of the hydraulic actuator to continuously measure the far-field applied displacement whilst a load cell measures the total shear force (i.e., the sum of that associated with the two individual fretting contacts). A summary of the fretting test parameters and conditions are presented in Table 2; these conditions were selected to deliver contact pressures and relative displacements representative of those experienced within aero-engine dovetail joints [10,15]. The specific value of 575 N was used for the normal load for consistency with our previous work [5,15,19], where this load was originally selected as it generates a contact pressure of 221 MPa, which enable comparison, with other published work [10]. It may be noted that the displacement amplitude used here is large compared to most fretting studies, however it is not out of line with other published work where fretting amplitudes of up to  $400 \mu\text{m}$  and  $500 \mu\text{m}$  respectively are used [24,25].

During the fretting tests, the tangential force and applied displacement were recorded at a rate of 200 times per fretting cycle; an assumption was made that the tangential force associated with each of the two fretting contacts was equal, and therefore the tangential force on each specimen was assumed to be a half of the total tangential force measured by the load cell. The tangential force-displacement data were plotted to form fretting loops of the type presented in Fig. 5. The coefficient of friction (CoF) ( $\mu$ ) is given by:

$$\mu = \frac{Q^*}{P} \quad (1)$$

where  $Q^*$  is the maximum tangential force per specimen recorded in each cycle and  $P$  is the constant normal load applied. Previous work looking at the behaviour of DFLs with this test geometry had shown that the CoF increased rapidly towards the end of the test and that this was associated with the failure of the coating system [15]. In light of that work, failure of a test pair in the current work was defined to have occurred when  $\mu \geq 0.7$  and for each material pairing type examined, tests to failure (i.e., to completion) were automatically terminated when that condition was first satisfied.

It is known that alongside the coefficient of friction itself, geometrical evolution of the contact also affects the maximum force recorded in a fretting cycle [26]. Accordingly, in this work, the energy coefficient of friction (ECof) ( $\mu_E$ ) [27] has been derived in post-test analysis of the data as follows:

$$\mu_E = \frac{E_d}{4P \delta^*} \quad (2)$$

where  $E_d$  is the energy dissipated over a fretting loop and  $\delta^*$  is the slip amplitude (as distinct from the applied displacement amplitude,  $\Delta^*$ ).

Once the number of cycles to failure of the various fretting pairing types had been determined, interrupted tests (i.e., tests which were stopped before failure took place) were conducted on selected sample pairing types from the test matrix. Such tests were conducted to facilitate a better understanding of the wear process in the various stages of fretting degradation of these systems by permitting examination of the

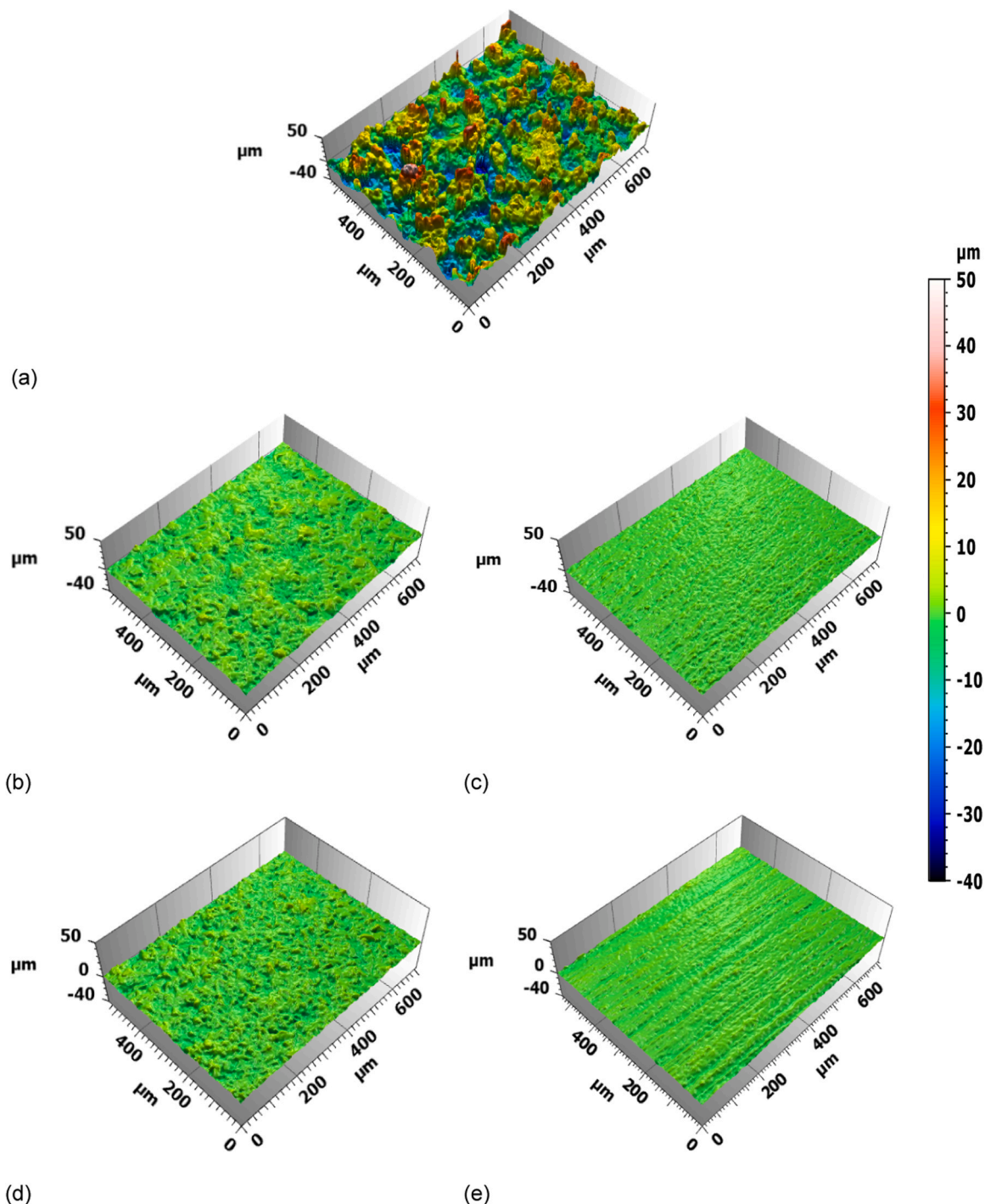


**Fig. 3.** Topographic 3D profiles of the flat Cu-Ni-In layer and Ti-6Al-4 V substrate surfaces prior to DFL coating application. (a) As-sprayed Cu-Ni-In, (b) Grit-blasted Cu-Ni-In, (c) Ground Cu-Ni-In, (d) Grit-blasted Ti-6Al-4 V, (e) Ground Ti-6Al-4 V.

samples prior to final failure.

Further 3D measurements (also with the Alicona system) were employed in this work to carry out surface profilometry of the wear scars from the flat and cylindrical specimens after fretting tests. Data from the Alicona system was processed using MountainsMap™. Before analysing the cylindrical samples, the surface form was first removed. From these measurements, average depth profiles across the scars were derived by taking the average of 50 individual profile lines across a scar.

After fretting tests, scanning electron microscopy (SEM) was utilised for the analysis of the wear scar features, using an FEI Quanta600 MLA SEM operating with an accelerating voltage of 20 kV. Wear scars were

examined both in plan-view and in cross-section; metallographic cross-sections were prepared by cold-mounting to ensure that potential degradation of the DFL that might have been associated with hot-mounting was avoided. Whole scar SEM cross-sections are presented with different magnifications in the horizontal and vertical directions to allow the characteristic features of the scars to be better presented to the reader; however, it is noted that this leads to image distortion of which the reader needs to be aware. Energy dispersive X-ray (EDX) analysis was performed in the SEM for quantitative chemical characterisation of the various features of the fretting wear scars.

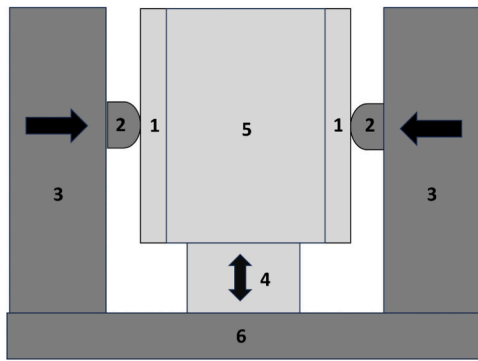


**Fig. 4.** Schematic diagram of the fretting setup. Static elements are dark grey, moving elements are light grey. (1) Ti-6Al-4 V flat specimen with contact length  $W = 10$  mm (2) Ti-6Al-4 V cylindrical specimen with radius  $R = 15$  mm (3) Fixed position hydraulic cylinder for applied normal load  $P = 575$  N (4) Vertical controlled actuator for applied displacement amplitude  $\Delta^* = 300$   $\mu\text{m}$  (5) Load cell (6) Mounting block.

**Table 2**  
Fretting test conditions employed.

Normal Load (P) / N	575
Displacement amplitude $\Delta^*$ / $\mu\text{m}$	300
Frequency (f) / Hz	2.5
Temperature (T) / $^{\circ}\text{C}$	$25 \pm 3$ (ambient)
Relative Humidity (%)	$30 \pm 5$ (ambient)

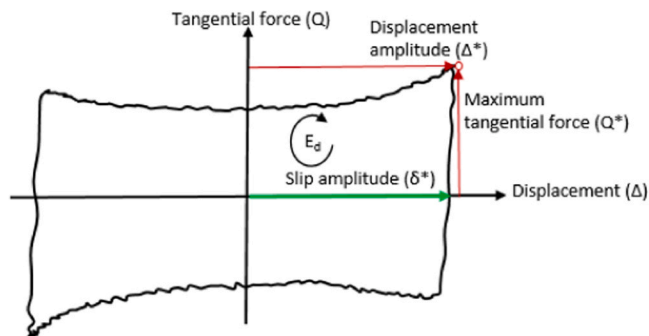


**Fig. 5.** Annotated schematic diagram of fretting loop.

### 3. Results

**Fig. 6** shows the cross-sectional BSE SEM images of representative different surfaces onto which the DFLs were deposited, along with information regarding the roughness of those surfaces derived from the Alicona measurements. Three distinct surface topographies have been generated for the Cu-Ni-In onto which the DFL was applied as shown in **Fig. 6a**, **b** & **c** (as-sprayed, ground and grit-blasted respectively). Two equivalent surface topographies have been generated for the Ti-6Al-4 V onto which the DFL was directly applied; as can be seen by comparison of **Fig. 6c** and **d**, the grit-blasted Ti-6Al-4 V has similar surface roughness and topographical features as that of the grit-blasted Cu-Ni-In surface. All three preparations exhibit a broadly symmetrical distribution of peaks and troughs. The as-sprayed Cu-Ni-In surface has the highest roughness and surface height parameters ranging from a peak of  $46$   $\mu\text{m}$  to a depth of  $-38$   $\mu\text{m}$ .

As can be seen in **Fig. 6a**, the DFL coating contours around the rough substrate (Cu-Ni-In) surface resulting in high variation in the DFL coating thickness on this substrate type. In some areas, a thin layer ( $\sim 25$   $\mu\text{m}$ ) of DFL exists when covering the high points of the surface and in other areas, a deposit with a much higher local DFL thickness exists, the

thickest of these being approximately  $60$   $\mu\text{m}$ .

#### 3.1. Effect of Cu-Ni-In interface roughness on system failure

The evolution of ECoF in the fretting wear tests conducted to failure where flat samples had the DFL applied to a Cu-Ni-In under-layer with the three different surface characteristics is presented in **Fig. 7a** (these tests were terminated when the CoF first exceeded  $0.7$ , although it is noted that the ECoF values are always much lower than that due to their averaging effect over the slip within any one cycle). It is seen that the DFL fretting lifetime increased with increasing surface roughness of the Cu-Ni-In under layer. A low friction coefficient ( $\text{ECoF} < 0.25$ ) is observed for the vast majority of the DFL lifetime of the system where the DFL was deposited onto the roughest (as-sprayed) Cu-Ni-In under-layer; in the case presented, a lifetime of  $615$  k cycles was observed. In the system where the DFL was deposited onto a grit-blasted Cu-Ni-In surface (GB Cu-Ni-In), a low ECoF of  $< 0.2$  was again observed soon after the beginning of the test; however, this low friction phase was short lived with the friction coefficient steadily increasing throughout the test with a significantly smaller number of fretting cycles to failure ( $229$  k cycles) being observed.

A significant difference in fretting behaviour was observed for the system where the DFL was deposited onto the smoothest (ground) Cu-Ni-In under-layer; no low friction phase was observed in the test, and instead the coefficient of friction rapidly rose until failure was reached after only  $69$  k cycles.

Profiles of the wear scars were made following tests to failure (i.e. when the CoF reached  $0.7$ ); **Fig. 7b** shows the maximum depths of the average profile of both the flat samples with the Cu-Ni-In layer with varying surface conditions and the mating cylindrical samples. The maximum depth at failure of the flat samples (i.e. the sample with the Cu-Ni-In interlayer) increased with increasing roughness of the Cu-Ni-In layer onto which the DFL was deposited. It is noted that the scars on the mating round specimens always exhibit a smaller depth of wear at failure than that of the flat counterpart; moreover, the ratio of the scar depth of the cylindrical and flat samples decreased as the lifetime of the pair increased (as the surface roughness of the Cu-Ni-In interlayer increased).

Typical, representative, cross sectional BSE SEM images of the flat Cu-Ni-In-coatings with the three different surface roughness following testing to failure are presented in **Fig. 8** (the reader is reminded of the different magnifications in the two directions in these images). **Fig. 8a** & **b** show the wear scars in the flat specimens with (i) the ground Cu-Ni-In layer with the lowest initial surface roughness ( $S_a$ ) of  $0.4$   $\mu\text{m}$  which failed at  $69$  k cycles and (ii) the grit-blasted Cu-Ni-In layer with a surface roughness ( $S_a$ ) of  $1$   $\mu\text{m}$  which failed at  $229$  k cycles. In these tests, failure occurred when the wear scar had penetrated only a small way ( $< \sim 50$   $\mu\text{m}$ ) into the Cu-Ni-In layer. In contrast, the wear scar in the specimen where the DFL had been applied onto an as-sprayed Cu-Ni-In with a high surface roughness ( $S_a$ ) of  $9$   $\mu\text{m}$  (which failed at  $615$  k cycles) indicated that much deeper penetration of the Cu-Ni-In layer had taken place when failure occurred.

For the system where the DFL was deposited onto the as-sprayed Cu-Ni-In layer, interrupted tests were also conducted. **Fig. 9a** show the evolution of ECoF from a test to failure and from an interrupted test which was stopped at  $200$  k cycles, which was judged to be still within the low friction phase. It is notable that the evolution of ECoF with exposure for the completed and interrupted test are very similar. **Fig. 9b** displays the accompanying wear depth profiles of the respective wear scars for the flat and round specimen where (i) the maximum depth of the averaged wear profile was around  $98$   $\mu\text{m}$  on the flat sample for the fully completed fretting test; (ii) the test stopped at  $200$  k cycles exhibited a wear depth of around  $36$   $\mu\text{m}$  on the flat sample. The Ti-6Al-4 V cylindrical counterpart of the interrupted test has a wear depth of  $23$   $\mu\text{m}$  whilst that from the completed test displays a wear depth of  $31$   $\mu\text{m}$ .

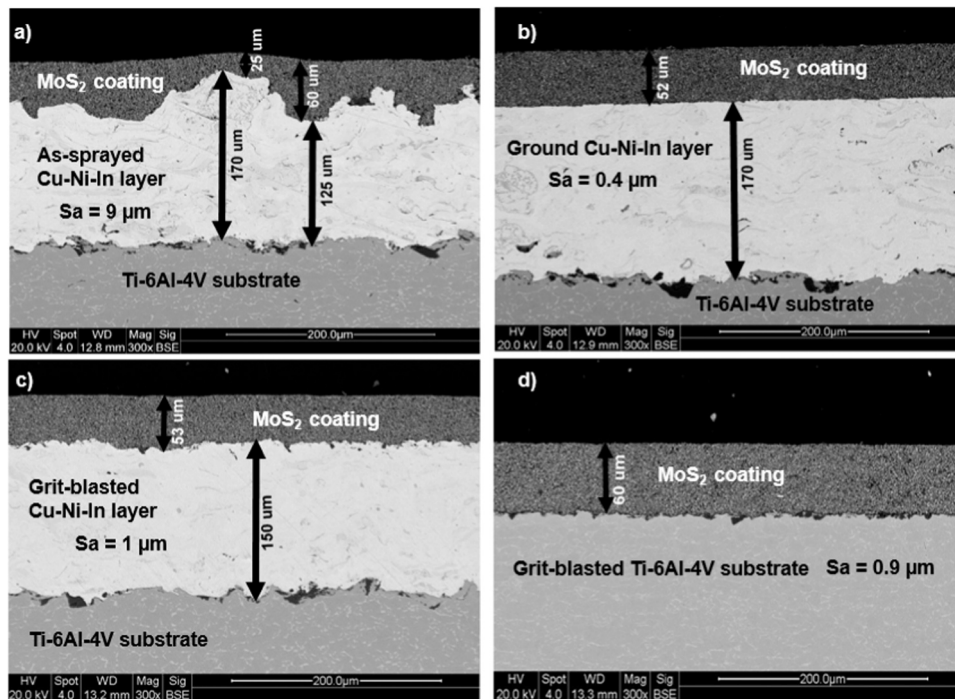


**Fig. 6.** Cross sectional BSE images of flat specimens with a layer of MoS<sub>2</sub> DFL coating before fretting test with the thickness measurements of layers as indicated. DFL deposited onto the following surface types: a) as-sprayed Cu-Ni-In layer, b) ground Cu-Ni-In layer, c) grit-blasted Cu-Ni-In layer, d) grit-blasted Ti-6Al-4 V.

The loss of DFL coating along with the extent of wear and damage which had occurred during the fretting wear test of the DFL deposited onto as-sprayed Cu-Ni-In layer can be seen in Fig. 10a which shows a cross sectional BSE SEM image of the fretting wear scar that had been interrupted during the low friction phase at 200 k cycles. Following 200 k cycles, the cross-sectional image (Fig. 10a) shows that very little wear of the Cu-Ni-In layer itself is observed; however, failure following 615 k cycles has resulted in much more significant penetration of the Cu-Ni-In interlayer (Fig. 10b).

Fig. 11a shows a plan-view BSE SEM image of the worn surface following interruption of the test with the as-sprayed Cu-Ni-In interlayer in the low friction regime (200 k cycles). The majority of the surface is made up of a dark-contrast region (the DFL) with small areas of bright-contrast (the Cu-Ni-In under-layer) being observed. The nature of the two regions is identified via EDX analysis. Despite the cylindrical body not having a Cu-Ni-In layer (i.e. being DFL deposited onto shot-peened Ti6Al-4 V), there is no evidence of titanium in the EDX analysis of either region on the surface of the flat specimens following these interrupted tests.

A high magnification cross sectional BSE-SEM image of the same surface from an interrupted test is presented in Fig. 11b. A thin layer is observed on the outer worn surface which was not observed in the samples prior to wear (see Fig. 6a); EDX analysis from these surface regions indicates a higher oxygen: molybdenum ratio than in the bulk of the DFL and provides evidence for formation of molybdenum oxide on the wearing surface as previously reported in the literature [5,21]. It is also noted that minimal Cu content exists in the outer surface layer which suggests the involvement of Cu-Ni-In asperities within the formation of the molybdenum oxide surface. Below this outer layer, an approximate DFL thickness of 20 – 30 μm remains within the deepest valleys of the rough Cu-Ni-In layer. Fig. 11 also shows areas in which the high Cu-Ni-In roughness peaks protrude through the DFL coating during the low friction stage, both in plan-view and in cross-section.

### 3.2. The effect of material type on system failure

In Fig. 12 a) Evolution of ECoF with number of cycles for fretting

tests to failure where the DFL was deposited onto either Ti-6Al-4 V or Cu-Ni-In, both with a ground or grit-blast surface condition, b) Maximum depths of the averaged wear profiles of the flat ground Ti-6Al-4 V and Cu-Ni-In and the flat grit-blasted Ti-6Al-4 V and Cu-Ni-In samples as well as their round shot peened Ti-6Al-4 V counterparts upon failure. a, the evolution of ECoF through the fretting tests are presented for systems where the DFL layer had been deposited onto both the Cu-Ni-In and Ti-6Al-4 V where the surfaces on to which the DFL had been deposited had two different topographies, namely that resulting from grinding and that resulting from grit-blasting. The relevant surface topographies can be seen in Fig. 3b & c and d & e for Cu-Ni-In and Ti-6Al-4 V surfaces respectively.

It can be seen that the material type has a strong effect on the lifetime of the systems for both topographies, with the Cu-Ni-In interlayer resulting in longer lifetimes than when the DFL was deposited onto Ti-6Al-4 V for both of the surface topographies examined. The data demonstrate the effect of material type on the system with different responses shown through the evolution of ECoF. In tests with the DFL deposited onto the grit-blasted Cu-Ni-In substrate, ECoF fell quickly to around 0.15 soon after the beginning of the test whereupon it remained stable for a duration of 20 k cycles. After this brief low friction phase, a gradual increase in ECoF was observed until failure was reached at 229 k cycles. In contrast, when the DFL was deposited onto grit-blasted Ti-6Al-4 V, the ECoF remained high throughout the test until failure was reached at only 45 k cycles.

The deposition of the DFL onto ground surfaces resulted in significantly reduced lifetimes compared to systems where the DFL had been deposited into grit-blasted surfaces. However, it is noted that again, ground Cu-Ni-In resulted in a much longer lifetime than ground Ti-6Al-4 V.

Fig. 12 a) Evolution of ECoF with number of cycles for fretting tests to failure where the DFL was deposited onto either Ti-6Al-4 V or Cu-Ni-In, both with a ground or grit-blast surface condition, b) Maximum depths of the averaged wear profiles of the flat ground Ti-6Al-4 V and Cu-Ni-In and the flat grit-blasted Ti-6Al-4 V and Cu-Ni-In samples as well as their round shot peened Ti-6Al-4 V counterparts upon failure. b shows the maximum depths of the averaged wear profiles of the fretting

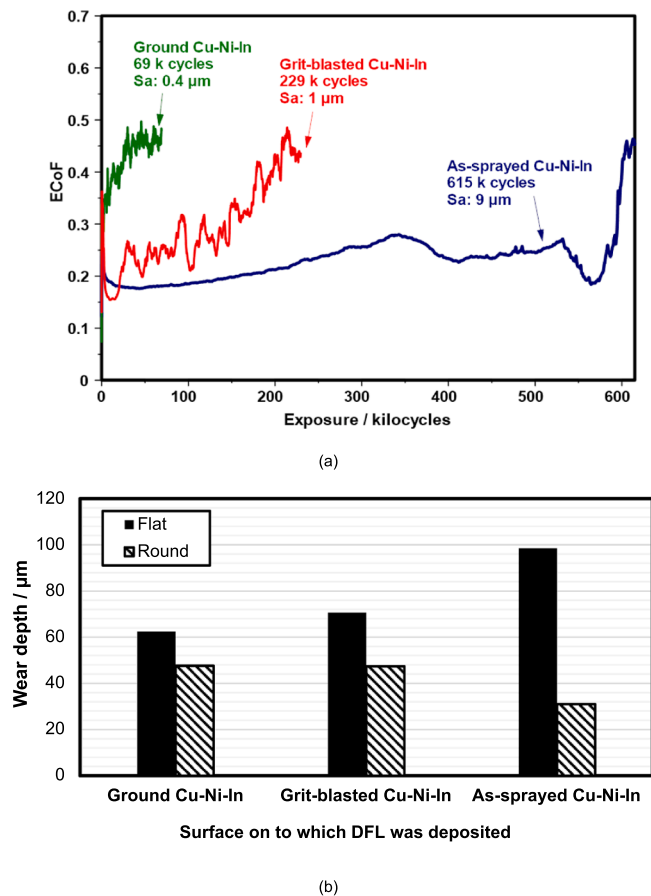


**Fig. 7.** a) Evolution of ECoF with number of cycles for fretting tests where flat samples had the DFL applied to the Cu-Ni-In layer with different surface preparations as indicated and the round counterpart was shot peened and DFL coated, b) Maximum depths of the averaged wear profiles (50 individual profiles used) at failure of the Cu-Ni-In coated flat samples and the shot peened Ti-6Al-4 V round samples following tests to failure.

wear scars from these tests. It is noted that the ground Cu-Ni-In has a deeper wear depth on the flat and the ground compared to the ground Ti-6Al-4 V. The fretting lifetime difference is however quite large as failure occurs at 3.7 k cycles on the ground Ti-6Al-4 V and at 69 k cycles on the ground Cu-Ni-In layer. The wear scar depth for the flat samples with the DFL deposited onto grit-blasted Cu-Ni-In was 70 μm whilst that of the flat sample where the DFL was deposited onto the grit-blasted Ti-6Al-4 V substrate was 139 μm. This depth range can be further observed in Fig. 13 where the cross-sectional BSE SEM wear scar images of the completed (worn to failure) tests for the flat grit-blasted Ti-6Al-4 V surface and the flat grit-blasted Cu-Ni-In surface are presented. For the grit-blasted Ti-6Al-4 V substrate (Fig. 13a), there is evidence of DFL delamination (a vertical step in the DFL itself, top right of Fig. 13a) which will have resulted in the protective influence of the DFL being curtailed. In contrast, the slope of the DFL in the Cu-Ni-In wear scar (Fig. 13b) indicates progressive wear of the DFL itself and the absence of early delamination.

## 4. Discussion

### 4.1. Effect of roughness of Cu-Ni-In under-layer

It is well known that the addition of a thermally sprayed Cu-Ni-In under-layer for the application of a DFL to Ti-6Al-4 V results in an extension to the durability of the DFL system. Whilst other studies ([14, 17,18]) have shown that an increase in roughness of a substrate to which

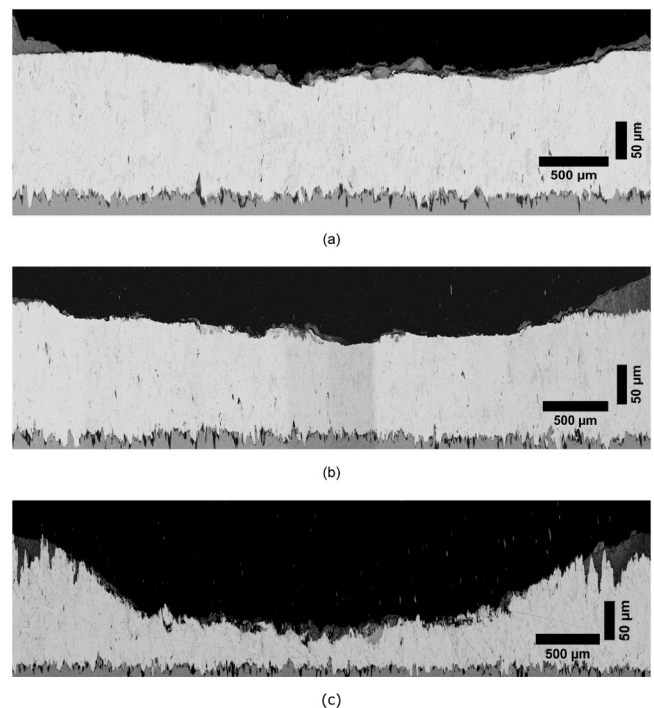


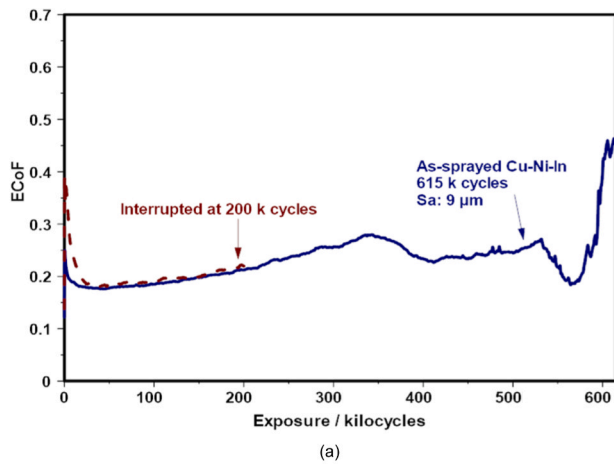
**Fig. 8.** Typical, representative, cross sectional BSE SEM fretting wear scar images of flat samples with a distorted aspect ratio (vertical magnification is six times larger than the horizontal magnification). (a) test with DFL which had been deposited onto ground Cu-Ni-In following completed test to failure at 69 kilocycles, (b) test with DFL which had been deposited onto grit-blasted Cu-Ni-In following completed test to failure at 229 kilocycles, (c) test with DFL which had been deposited onto as-sprayed Cu-Ni-In following completed test to failure at 615 kilocycles.

a DFL is applied results in an extension of DFL system lifetime, this has tended to be in the range of roughness (Sa) values up to around ~3 μm. In this work, the roughness of as-sprayed Cu-Ni-In has been modified by further preparation and the same increase in DFL lifetime was again observed with increasing roughness (Fig. 7a).

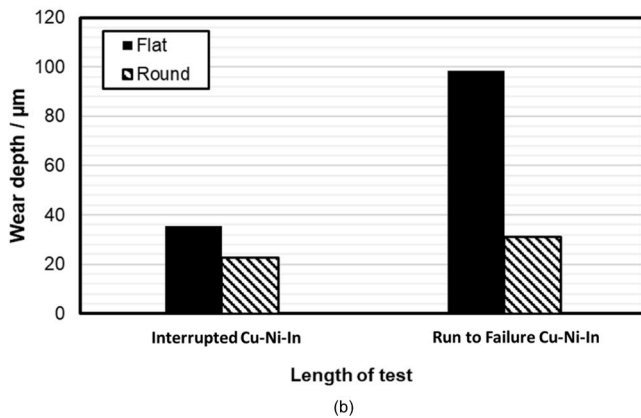
Previous work using the same cylinder-on-flat contact geometry has examined the behaviour of a systems where the DFL was deposited on to a grit-basted Ti-6Al-4 V substrate [15]. A general form of evolution of ECoF with exposure was observed and was categorised into three stages as indicated in Fig. 15. The following explanation was proposed: Stage I (with a high but falling ECoF) was associated with wear of the DFL itself; Stage II (where the ECoF fell rapidly and then remained relatively low and steady) was associated with wear of the mixed metal-DFL layer; Stage III was initiated when the DFL was exhausted and was associated with metal-metal contact and both instabilities with a generally rapid rise in the ECoF.

In this context, it is notable that when the DFL was deposited onto ground Cu-Ni-In (Sa ~ 0.4 μm), there was no evidence of Stages I or II in the evolution of ECoF with exposure, with behaviour similar to Stage III from the outset (Fig. 7a) characterised by a rising ECoF with significant instability. As such, it is proposed that the DFL delaminates in this case and so it is neither worn away (Stage I absent) nor does any mixed DFL-metal layer form (Stage II absent). The fact that the DFL delaminates indicates that one of the functions of a rough surface is to provide a mechanical key for the retention of the DFL.

For the system where the DFL had been deposited onto the grit-blasted Cu-Ni-In (Sa ~ 1.0 μm), Stage I appeared to be absent (or very short) with Stage II being maintained until around  $25 \times 10^3$  cycles (Fig. 7a). In this case, Stage III was maintained until an exposure of  $229 \times 10^3$  cycles; it is notable that this is much longer than the Stage III in the system where it is proposed that the DFL delaminated (where the

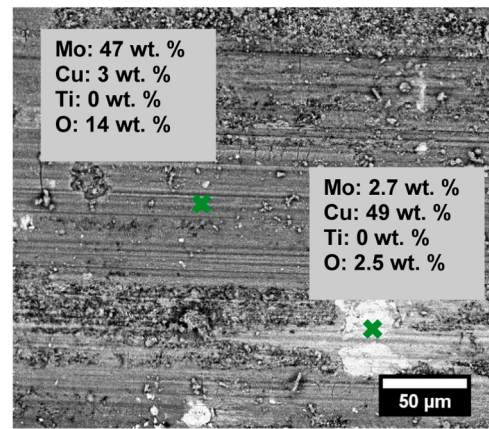


(a)

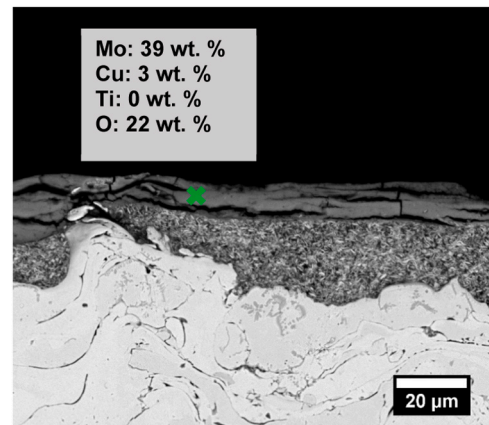


(b)

Fig. 9. a) Evolution of ECoF with number of cycles for as-sprayed Cu-Ni-In fretting wear test which were interrupted and run to failure; b) Maximum depths of averaged wear profiles (50 individual profiles used) of as-sprayed flat Cu-Ni-In sample and the shot peened cylindrical Ti-6Al-4 V samples of tests that were (i) interrupted at 200 k cycles and (ii) run to failure at 615 k cycles.



(a)



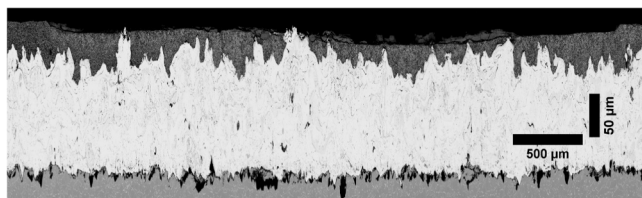
(b)

Fig. 11. BSE SEM images of fretting wear scars of a test where the DFL was deposited on an as-sprayed Cu-Ni-In flat sample that was interrupted at 200 k cycles a) plan view high magnified area, b) cross-section high magnified area.

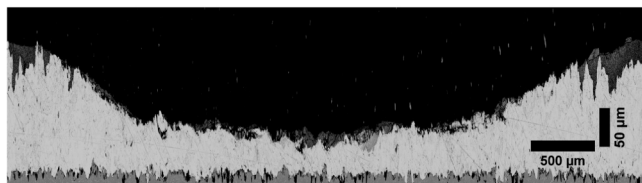
surface ( $S_a = 9 \mu\text{m}$ ), no Stage I was seen again, but the low friction (Stage II) phase lasted at least ten times longer (although it is recognised that it is not clear when Stage II ends and Stage III begins in this case).

Together, these observations therefore strengthen the conclusions drawn in earlier work [5] that the mixed DFL-metal layer is both durable and confers low friction in Stage II, and that its formation and maintenance is best achieved by a high roughness metal onto which the DFL is deposited. A surface of sufficient roughness is required to act as a mechanical key for the DFL and thus prevent its delamination; if this is not achieved, low system durability is observed. The reason for the lack of Stage I behaviour with this system is not clear.

This durable nature of the mixed metal -DFL material is demonstrated by the cross-section of the test sample which was interrupted following  $200 \times 10^3$  cycles (Fig. 10a); here, despite the number of cycles being around a third of those resulting in system failure, the majority of the thickness of the DFL itself has been worn away (Fig. 9b) but there is very little penetration and damage of the Cu-Ni-In under-layer itself. The plan view image (Fig. 11a) shows Cu-Ni-In providing support on the surface whilst the higher magnification cross-section in Fig. 11b indicates the formation of a surface layer on top of the DFL; this upper glaze layer is rich in both molybdenum and oxygen but also contains copper, indicating that the Cu-Ni-In layer is involved to some limited degree in the formation of this upper glaze layer. The significant roughness in the as-sprayed Cu-Ni-In coating as well as the even distribution of high peaks and deep pits across the surface (Figs. 3a and 6a) provide reservoirs for the DFL which replenish the durable and low friction mixed metal - DFL layer as it is worn away.



(a)

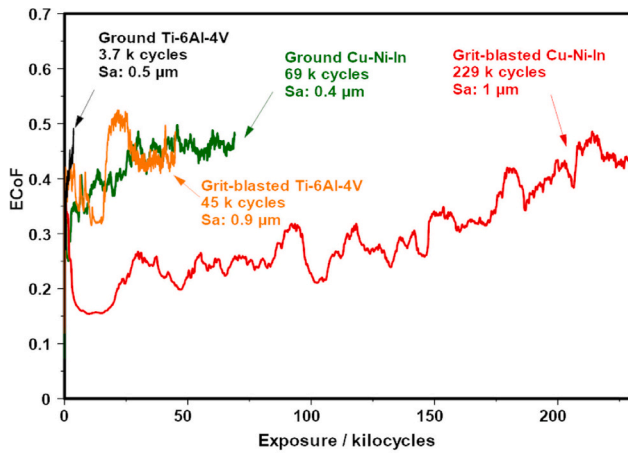


(b)

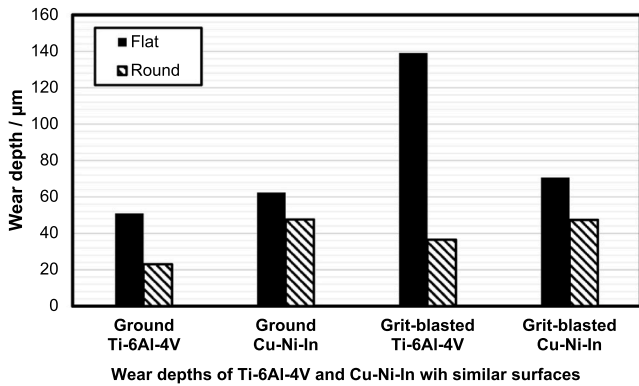
Fig. 10. Typical, representative, cross sectional BSE SEM fretting wear scar images of flat samples with a distorted aspect ratio (vertical magnification is six times larger than the horizontal magnification). (a) test with DFL which had been deposited onto as-sprayed Cu-Ni-In following a test that was interrupted at 200 k cycles, (b) test with DFL which had been deposited onto as-sprayed Cu-Ni-In following completed test to failure at 615 k cycles.

DFL was applied to a ground surface) and it is therefore proposed that some of the DFL must be retained into Stage II to effect that difference. Finally, when the DFL was deposited onto the as-sprayed Cu-Ni-In



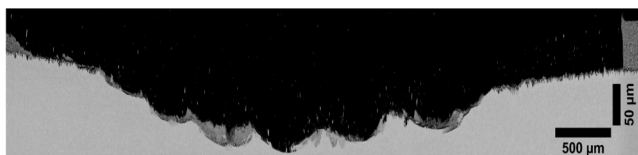


(a)

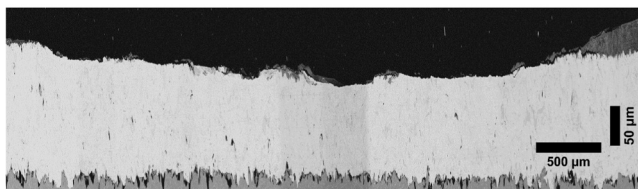


(b)

**Fig. 12.** a) Evolution of ECoF with number of cycles for fretting tests to failure where the DFL was deposited onto either Ti-6Al-4 V or Cu-Ni-In, both with a ground or grit-blast surface condition, b) Maximum depths of the averaged wear profiles (50 individual profiles used) of the flat ground Ti-6Al-4 V and Cu-Ni-In and the flat grit-blasted Ti-6Al-4 V and Cu-Ni-In samples as well as their round shot peened Ti-6Al-4 V counterparts upon failure.

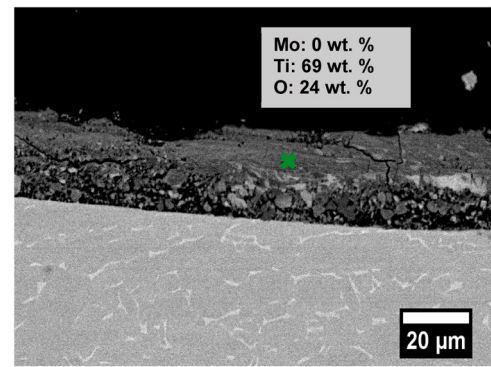


(a)

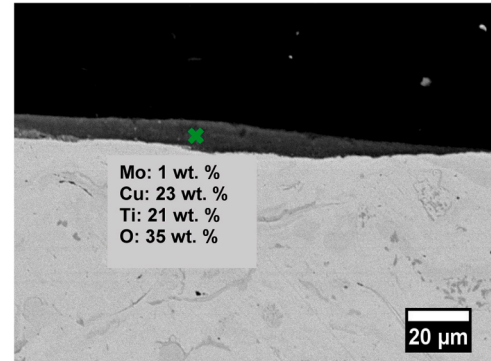


(b)

**Fig. 13.** Typical, representative, cross sectional BSE SEM fretting wear scar images of flat samples with a distorted aspect ratio (vertical magnification is six times larger than the horizontal magnification). (a) test with DFL which had been deposited onto grit-blasted Ti-6Al-4 V following completed test to failure at 45 k cycles, (b) test with DFL which had been deposited onto grit-blasted Cu-Ni-In following completed test to failure at 229 k cycles.



(a)



(b)

**Fig. 14.** High magnification cross sectional BSE SEM images of flat samples from fretting wear scars, along with EDX analysis: a) test with DFL which had been deposited onto grit -blasted Ti-6Al-4 V substrate upon failure at 45 k cycles, b) test with DFL which had been deposited onto grit-blasted Cu-Ni-In layer upon failure at 229 k cycles.

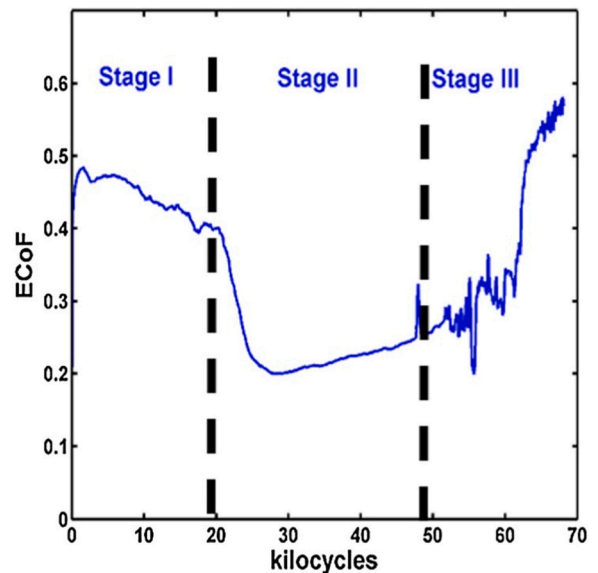


**Fig. 15.** Diagram categorising the evolution of ECoF into three stages of behaviour (from [15]).

Once the durable Cu-Ni-In – DFL mixed material has been removed, the Cu-Ni-In wears rapidly and wears much more rapidly than the Ti-6Al-4 V. Fig. 9b shows that after 200 kilocycles of exposure, the cylinder (which was originally made up of DFL deposited onto a shot-peened Ti-6Al-4 V surface) has worn to a depth of ~ 23 μm whereas the flat

specimen (with its Cu-Ni-In under-layer) has a worn to a depth of 36  $\mu\text{m}$ . As the number of cycles of exposure were increased to generate system failure, the worn depth of the cylindrical specimen increased by  $\sim 5 \mu\text{m}$ , whereas the worn depth of the Cu-Ni-In containing flat sample increased by  $\sim 60 \mu\text{m}$ . This preferential wear of the Cu-Ni-In can be attributed to its low hardness compared to the Ti-6Al-4 V ( $177 \pm 20 \text{ HV}$  and  $287 \pm 10 \text{ HV}$  respectively).

As well as extending the lifetime, the increased roughness of the Cu-Ni-In under-layer also resulted in an increase in the depth of wear of the Cu-Ni-In coated flat specimen before  $\text{CoF} > 0.7$  (the measure of test failure and the signal for the test to be stopped) and a decrease in the plain Ti-6Al-4 V round specimen (Fig. 7). Fig. 8 shows that for all three of the Cu-Ni-In surface topographies examined, the depth of wear into the Cu-Ni-In when failure was deemed to have occurred was very much larger than the scale of the surface roughness, implying that the effect of the DFL is experienced long after the original thickness of the DFL has been worn away.

#### 4.2. Comparison between Cu-Ni-In and Ti-6Al-4 V with similar roughnesses

Whilst it has been shown that the roughness of as-sprayed Cu-Ni-In is a key factor in extending the lifetime of the DFL, there is a need to understand if this is simply a roughness effect or if there is a dependence upon the material type. In this work, the surface of the as-sprayed Cu-Ni-In coating was further modified to be directly comparable to the topographies of Ti-6Al-4 V in both the ground and grit-blasted conditions. The similar nature of the surface topography of both Cu-Ni-In and Ti-6Al-4 V in a smooth ground state and with a grit-blasted surface condition (as displayed in Figs. 3 and 6) has allowed the effect of these two substrate materials on test duration and failure mode to be examined independently of the effects of topography.

The evolution of ECoF with exposure to wear for the four surface types (two materials and two roughnesses) is presented in Fig. 12. Significant differences in behaviour are observed for the systems where the DFL was applied to a Ti-6Al-4 V substrate as was seen when it was applied to the Cu-Ni-In.

When the DFL was applied to the ground Ti-6Al-4 V ( $S_a \sim 0.5 \mu\text{m}$ ), no stage I or Stage II behaviour was seen, with the system failing after just  $3.7 \times 10^3$  cycles. This again indicates that the DFL delaminated from the substrate due to the lack of a mechanical key between them. In contrast, when the DFL was deposited onto a grit-blasted Ti-6Al-4 V substrate ( $S_a \sim 0.9 \mu\text{m}$ ), Stage I behaviour was observed (with a duration of  $\sim 10 \times 10^3$  cycles) indicating that the DFL was worn through rather than delaminated. A short period of Stage II behaviour was then observed before Stage III commenced. For the grit-blasted systems, the wear scar depth (Fig. 12b) for the grit-blasted Ti-6Al-4 V-based system was very much larger than the DFL thickness itself ( $\sim 140 \mu\text{m}$ ) whereas for the Cu-Ni-In based system, failure occurred soon after the thickness of the DFL had been exceeded. This significant difference can also be observed in the cross-sectional micrographs presented in Fig. 13. Higher magnification images (with EDX analysis) of cross-sections of the surfaces of the two grit-blasted systems following failure (Fig. 14) show that in the case of the Ti-6Al-4 V surface, there is no evidence of the DFL when failure occurred (i.e. no molybdenum is detected) whereas molybdenum was still present in the surface layer present when failure of the Cu-Ni-In system occurred. It is also notable in this latter case that titanium was present in the surface layer; this titanium must have come from the counter-body indicating that the DFL had been penetrated there also. The greater wear depth at failure with the Ti-6Al-4 V system compared to the system with Cu-Ni-In has been observed in previous studies [5]. Niu et al. [8] credited the low depth of the Cu-Ni-In layer to delamination wear which under fretting, generates soft and large flake debris that could be easily retained in the contact area to form a third body. The effective load carrying capacity of the debris effectively inhibited the damage of the Cu-Ni-In coated specimen.

The systems where the DFL was deposited onto Ti-6Al-4 V exhibited much lower durability than those where the DFL was deposited onto Cu-Ni-In with a similar topography. In the cases where it is proposed that delamination of the DFL occurred (i.e. where the DFL was deposited onto a ground surface), it is seen that Stage III (i.e. where ECoF rises steadily towards failure) lasts almost twenty times longer in the system with the Cu-Ni-In under-layer. In the cases where the DFL was deposited onto a grit-blasted surface, both Stage II and Stage III were much longer for the system with the Cu-Ni-In under-layer with a lifetime extension of approximately five times with the Cu-Ni-In under-layer.

Together, this evidence indicates that the Cu-Ni-In provides an extension to the lifetime in this system compared to Ti-6Al-4 V. Although previous studies [6–8] have shown similar friction coefficients occur for unlubricated self-mated Ti-6Al-4 V, and plasma sprayed Cu-Ni-In coatings mated against Ti-6Al-4 V counter-body when deployed without any DFL. In the case considered in the current work, it must be remembered that the counter-body in all cases was a shot-peened Ti-6Al-4 V surface to which a DFL had been applied. As such, it is argued here that in light of the observations made in the literature, the enhanced lifetimes associated with the inclusion of Cu-Ni-In in the system do depend upon the presence of a DFL on at least one of the surfaces. However, the fact that the lifetimes of both the Ti-6Al-4 V and the Cu-Ni-In were significantly longer if the DFL was deposited onto a grit-blasted surface rather than a ground surface indicates that the effect of the DFL being retained by the surface roughness is critical to lifetime extension in both cases.

## 5. Conclusion

In this study, the effects of the interfacial geometry and material type upon which a polymer bonded  $\text{MoS}_2$  based DFL is deposited on is investigated and has permitted further understanding of the working mechanisms that enables the extension of fretting lifetimes and durability of the bonded DFL coating systems. By modifying the interfacial roughness of the as-sprayed Cu-Ni-In under-layer, the increase of DFL fretting lifetimes and system durability was found to correlate with increased surface roughness. The surface of the underlying Cu-Ni-In coating was modified to be directly comparable to the Ti-6Al-4 V substrate in both the ground and grit-blasted conditions. With this, the material effects of the DFL coated fretting system could be isolated. The experimental results showed that:

- In both the smooth ground state and grit-blasted conditions, samples with a Cu-Ni-In under-layer showed better durability and lifetimes when compared to Ti-6Al-4 V substrate despite having similar surface topographies.
- The interfacial surface roughness plays a key role in enabling the formation of a low ECoF mixed metal-DFL phase which, regardless of material type, enhances fretting lifetime.
- The roughness of as-sprayed Cu-Ni-In is a key factor in extending the lifetime of the DFL which is proposed to provide a mechanical key for the retention of the DFL to prevent delamination of the DFL coating and increase system durability.
- When a thermally sprayed Cu-Ni-In layer is used in its as-sprayed condition, these effects of high roughness and material durability combine to significantly enhance the fretting lifetime compared to a non-roughened Ti-6Al-4 V surface.
- For the results presented here, the change in material from Ti-6Al-4 V to Cu-Ni-In at a fixed surface roughness of 0.9–1  $\mu\text{m}$  increased fretting lifetime by approximately fivefold. Increasing roughness of the Cu-Ni-In layer from 1  $\mu\text{m}$  to 9  $\mu\text{m}$  more than doubled fretting lifetime.

Further work to determine the optimum surface would need to include a cost benefit analysis of the relevant surface engineering

processes. Scratch and adhesion tests could also be carried out to increase understanding of how such surface modification impacts the overall performance of the coating systems. Use of EPMA, Electron Probe MicroAnalysis, could also be included in future work in order to gain more detailed insight into the composition of the different phases present in the wear scars.

### Declaration of Competing Interest

The authors declare that they have no known competing financial interests or personal relationships that could have appeared to influence the work reported in this paper.

### Data availability

The data that has been used is confidential.

### Acknowledgements

The work presented in this paper formed part of Emmanuel Laolu-Balogun's PhD "The Effect of Fretting Conditions on the Lifetime of Aero-engine Dry Film Lubricant Systems" which was funded by Rolls-Royce plc and the EPSRC via an industrial CASE award EPSRC DTP (Case Conversion) grant ref. EP/N50970X/1.

### References

- [1] Luo DB, Fridrici V, Kapsa P. Relationships between the fretting wear behavior and the ball cratering resistance of solid lubricant coatings. *Surf Coat Technol* 2010;vol. 204(8):1259–69.
- [2] Waterhouse RB, Shipway PH. Fretting wear. *Frett Wear* 2007.
- [3] Wei DS, Wang YR. Analysis of fretting fatigue life of dovetail assemblies based on fracture mechanics method. *Eng Fail Anal* 2012;vol. 25:144–55.
- [4] Yang Q, et al. Investigation of shot peening combined with plasma-sprayed CuNiIn coating on the fretting fatigue behavior of Ti-6Al-4V dovetail joint specimens. *Surf Coat Technol* 2019;vol. 358:833–42.
- [5] Barman K, Shipway PH, Voisey KT, Pattinson G. The role of a thermally sprayed CuNiIn underlayer in the durability of a dry-film lubricant system in fretting – A phenomenological model. *Tribol Int* 2018;vol. 123:307–15.
- [6] Hager CH, Sanders J, Sharma S, Voevodin A. Gross slip fretting wear of CrCN, TiAlN, Ni, and CuNiIn coatings on Ti6Al4V interfaces. *Wear* 2007;vol. 263(1–6 SPEC. ISS):430–43.
- [7] Fridrici V, Fouvry S, Kapsa P. Fretting wear behavior of a Cu–Ni–In plasma coating. *Surf Coat Technol* 2003;vol. 163–164:429–34.
- [8] Niu Z, Zhou W, Wang C, Cao Z, Yang Q, Fu X. Fretting wear mechanism of plasma-sprayed CuNiIn coating on Ti-6Al-4V substrate under plane/plane contact. *Surf Coat Technol* 2021;vol. 408(August 2020):126794.
- [9] Kim K, Korsunsky AM. Dissipated energy and fretting damage in CoCrAlY-MoS2 coatings. *Tribol Int* 2010;vol. 43(3):676–84.
- [10] Kim K, Korsunsky AM. Effects of imposed displacement and initial coating thickness on fretting behaviour of a thermally sprayed coating. *Wear* 2011;vol. 271(7–8):1080–5.
- [11] Sabeya GRYN, Paris J-Y, Denape J. Fretting wear of a coated titanium alloy under free displacement. *Wear* 2008;vol. 264(3–4):166–76.
- [12] Mary C, Fouvry S, Martin JM, Bonnet B. Pressure and temperature effects on Fretting Wear damage of a Cu–Ni–In plasma coating versus Ti17 titanium alloy contact. *Wear* 2011;vol. 272(1):18–37.
- [13] Xu J, Zhou ZR, Zhang CH, Zhu MH, Luo JB. An investigation of fretting wear behaviors of bonded solid lubricant coatings. *J Mater Process Technol* 2007;vol. 182(1–3):146–51.
- [14] Zhu MH, Zhou ZR. An investigation of molybdenum disulfide bonded solid lubricant coatings in fretting conditions. *Surf Coat Technol* 2001;vol. 141(2–3):240–5.
- [15] Barman K, Shipway PH, Voisey KT, Pattinson G. Evolution of damage in MoS2-based dry film lubricants (DFLs) in fretting wear—The effect of DFL thickness and contact geometry. *Prog Org Coat* 2017;vol. 105:67–80.
- [16] Luo DB, Fridrici V, Kapsa P. Selecting solid lubricant coatings under fretting conditions. *Wear* 2010;vol. 268(5–6):816–27.
- [17] Luo DB, Fridrici V, Kapsa P. Evaluating and predicting durability of bonded solid lubricant coatings under fretting conditions. *Tribol Int* 2011;vol. 44(11):1577–82.
- [18] Xu J, Zhu M, Zhou Z, Kapsa P, Vincent L. An investigation on fretting wear life of bonded MoS2 solid lubricant coatings in complex conditions. *Wear* 2003;vol. 255(1–6):253–8.
- [19] E. Laolu-Balogun, S.P. Owen, S. Read, G. Pattinson, P.H. Shipway, and K.T. Voisey, Effects of Ti-6Al-4V Surface Condition on the Performance of DFL Lifetimes, in *Proceedings of the 8th International Conference on Fracture, Fatigue and Wear*, 2021, pp. 657–672.
- [20] Fridrici V, Fouvry S, Kapsa P, Perruchaut P. Impact of contact size and geometry on the lifetime of a solid lubricant. *Wear* 2003;vol. 255(7–12):875–82.
- [21] Fouvry S, Paulin C. An effective friction energy density approach to predict solid lubricant friction endurance: Application to fretting wear. *Wear* 2014;vol. 319(1–2):211–26.
- [22] Yang Q, et al. Effect of shot-peening on the fretting wear and crack initiation behavior of Ti-6Al-4V dovetail joint specimens. *Int J Fatigue* 2018;vol. 107 (September 2017):83–95.
- [23] Kirk D. Shot peening. *Aircr Eng Aerosp Technol Int J* 1999;vol. 77(4):349–61.
- [24] Liu QY, Zhou ZR. Effect of displacement amplitude in oil-lubricated fretting. *WEAR* 2000;vol. 239:237–43.
- [25] Kalin M, Vizintin J. The tribological performance of DLC coatings under oil-lubricated fretting conditions. *Tribol Int* 2006;vol 39:1060–7.
- [26] Jin X, Sun W, Shipway PH. Derivation of a wear scar geometry-independent coefficient of friction from fretting loops exhibiting non-Coulomb frictional behaviour. *Tribol Int* 2016;vol. 102:561–8.
- [27] Fouvry S, Duó P, Perruchaut P. A quantitative approach of Ti-6Al-4V fretting damage: Friction, wear and crack nucleation. *Wear* 2004;vol. 257(9–10):916–29.